PERFORMANCE OF A PILE-SUPPORTED HIGHWAY EMBANKMENT OVER SOFT GROUND REINFORCED WITH GEOSYNTHETICS

D.S. Liyanapathirana[1], H.G. Poulos[2] and C.Leo[1]
[1] *School of Engineering, University of Western Sydney, Locked Bag 1797, Penrith South DC, NSW, Australia 1797*
[2] *Coffey Geotechnics, 8/12 Mars Road, Lane Cove West, NSW, Australia 2066*

ABSTRACT

In this paper, a case history of a geosynthetic reinforced pile-supported embankment over soft clay is numerically simulated using a fully coupled finite element analysis. Field monitored data for pressures transferred from the embankment to the piles and soft foundation soil, excess pore pressures, settlements of piles and soil, and lateral deformations are compared with results from the finite element analysis. Results show that a significant amount of embankment load is carried by the piles and hence the excess pore pressures generated in the foundation soil are remarkably low. Although lateral effects are not usually incorporated in design methods used in current practice, results show that they are significant closer to the toe of the embankment.

1 INTRODUCTION

Due to low bearing capacity and excessive settlement characteristics of soft soils, geotechnical engineers dealing with embankment construction over soft ground encounter a real challenge. As a result, a wide range of technologies has been developed to support embankments on soft ground. Although vertical drains and preloading can be used to mitigate unfavourable characteristics of soft soils, it is often not economical to allow the soil to gain stiffness and strength through consolidation due to time constraints and uncertainty of soil conditions. Therefore, alternative innovative construction technologies are needed. One such solution is geosynthetic reinforced pile-supported embankments, which is an attractive sustainable technology for 'fast-track' construction environments.

The inclusion of geosynthetics in pile-supported embankments has several advantages. It significantly improves the efficiency of load transfer to the piles and minimises the yielding of the soil above pile heads. The load transferred to the piles may be increased by the vertical component of the tension in the geosynthetic. It also potentially reduces the total and differential settlements which can be reflected to the surface of the embankment. Since pile spacing can be increased with the inclusion of geosynthetics, significant cost reductions can be achieved compared with conventional pile-supported embankments (Han and Akins, 2002).

Since the early 1980s, several theoretical methods (e.g. finite element method, finite difference method and analytical solutions based on principles of soil mechanics) and experimental studies have been carried out around the world to better understand the role of geosynthetics on the load transfer mechanism. In a majority of currently available design methods it is assumed that the embankment load is transferred to the piles by the soil arching effect described by Terzaghi (1943) based on his classical trap door experiment. For the pile-supported embankment systems, Hewlett and Randolph (1988) carried out model tests and observed the formation of "vaults" across adjacent pile caps and developed expressions to obtain the load carried by piles. This method seems to be by far the most successful and is therefore one of the routinely used design methods. In the design it is assumed that the proportion of the embankment load that has not arched on to the pile caps is supported by the geosynthetic but the lateral effects have not been taken into account. Therefore this method provides a lower bound for the proportion of load transferred to the piles in geosynthetic reinforced pile-supported embankments.

The proportion of the vertical load carried by the geosynthetic should be a function of the stiffness of the geosynthetic as well as the modulus of the piles below the embankment. However, the closed form solutions proposed by Jones *et al*. (1990), Guido *et al*. (1987) and Rogbeck *et al.* (1998) have ignored this parameter. The design procedure recommended in British Standard for strengthened/reinforced soils and other fills (BS8006:1995) is the method developed by Jones *et al*. (1990). In this method the average pressure acting on the pile caps has been computed based on the loading of an infinitely long pipe in a two-dimensional situation, which differs from the usual practice with square pile caps. In addition, Love and Milligan (2003) proved that this method does not satisfy vertical equilibrium. Low *et al.* (1994) proposed equations incorporating the stiffness of the geosynthetic and validated their equations using small scale laboratory model tests. They used cap beams in the transverse direction. Since this arrangement differs from the usual

practice, the application of this method is limited. Another problem with their method is that they used soft rubber foam to simulate the soft foundation soil, where the stress conditions in the model are much smaller than the stress conditions in the field.

In the present study, a fully coupled two-dimensional plane strain finite element analysis has been used to analyse a case history of a geosynthetic reinforced pile-supported embankment. The site is located in northern Shanghai, China. The deformation characteristics of the piled embankment are investigated at the end of embankment construction and 400 days after the construction when the deformations due to consolidation are complete. The computed results are discussed and compared with field measurements reported by Liu *et al.* (2007). In addition, the load transfer from the embankment to the geosynthetic computed from the finite element method is compared with design methods proposed in BS8006, Terzaghi (1943), Hewlett and Randolph (1988) and Guido *et al.* (1987).

2 DETAILS OF EMBANKMENT AND SITE CONDITIONS

Figure 1 shows the soil profile and the cross section of the instrumented test embankment. The ground water level is at 1.5 m below the ground surface. The embankment was supported by concrete piles with outer diameter of 1.0 m. Piles were 16 m long and founded on the sandy silt layer, which is relatively stiff compared to the silty clay layers above. The top 0.5 m of the pile section was a solid cylindrical section but the rest of the pile section was a pipe section with a wall thickness of 120 mm. The centre to centre distance between piles was 3 m.

Above the pile heads a 0.25 m thick well graded, gravel layer was placed to provide a working layer and to avoid damage of the geosynthetic above the pile heads (Liu *et al.*, 2007). Another 0.25 m thick gravel layer was placed above the geosynthetic layer, making the total thickness of the gravel layer above the pile heads 0.5 m.

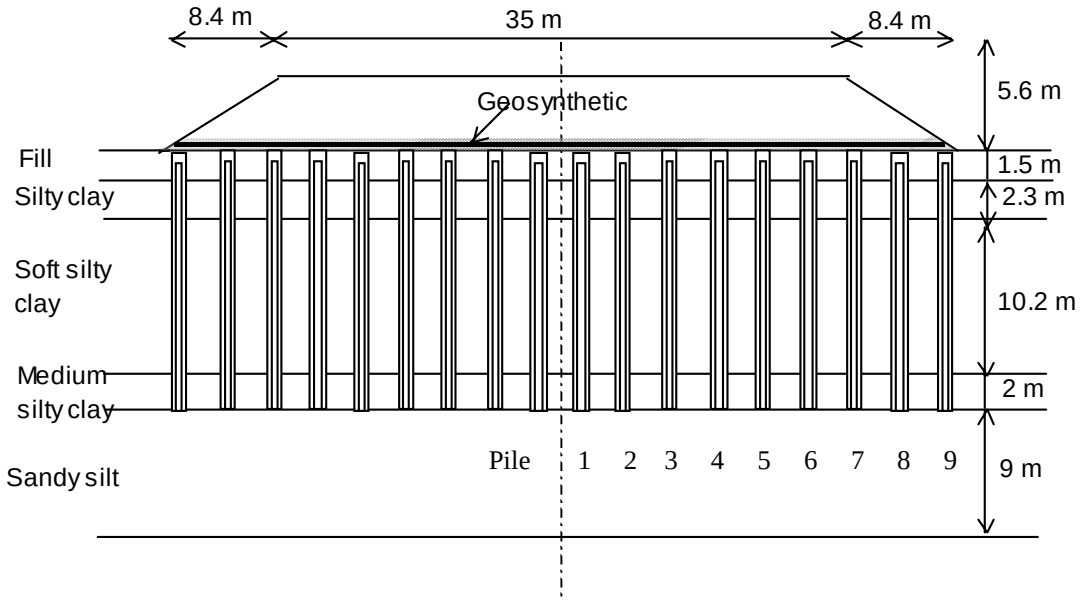

Figure 1: Cross section of the geosynthetic reinforced pile-supported highway embankment.

3 NUMERICAL MODEL

Figure 2 shows the finite element model used for the analysis. By taking into account the symmetry of the problem only one half of the embankment was analysed assuming plane strain conditions. The numerical model was based on the coupled theory of nonlinear porous media and finite element analysis was carried out using ABAQUS/ Standard. This allowed investigation of excess pore pressure generation during the embankment construction and subsequent excess pore pressure dissipation during consolidation. The constitutive behaviour of the four silt layers was modelled using the Modified Cam Clay model, which requires six material parameters: slope of the virgin consolidation line, λ; slope of the swelling line, κ; the void ratio at unit pressure, e_1; slope of the critical state line, M; Poisson's ratio, ν.

The embankment was constructed to a height of 5.6 m in ten lifts over a period of 55 days and the history of embankment construction is shown in Figure 3. Normally embankment fill materials have a relatively high permeability. Therefore, the fill material was assumed to behave in a drained manner. The constitutive behaviour of the fill material and gravel layers are modelled using a linear elastic-perfectly plastic model with a Mohr-Coulomb failure criterion, which requires five parameters: effective cohesion, c'; friction angle, ϕ'; dilatancy angle, ψ'; Young's modulus, E and Poisson's ratio, ν.

Piles and Geosynthetic reinforcement were modelled as linear elastic materials. The parameters used in the analyses are summarised in Table 1. Both soil and piles were modelled using eight-node quadrilateral elements and the geosynthetic was modelled as a cable, which can carry only tension.

In the first increment block of the analysis, the finite element mesh corresponding to embankment was removed and an initial stress state was established in the foundation soil based on the unit weight of each soil layer. Then the embankment construction was simulated by adding a set of elements corresponding to each lift of the fill material within a duration of 5.5 days. After adding ten lifts of the fill material, the foundation soil was allowed to consolidate for a period of 400 days.

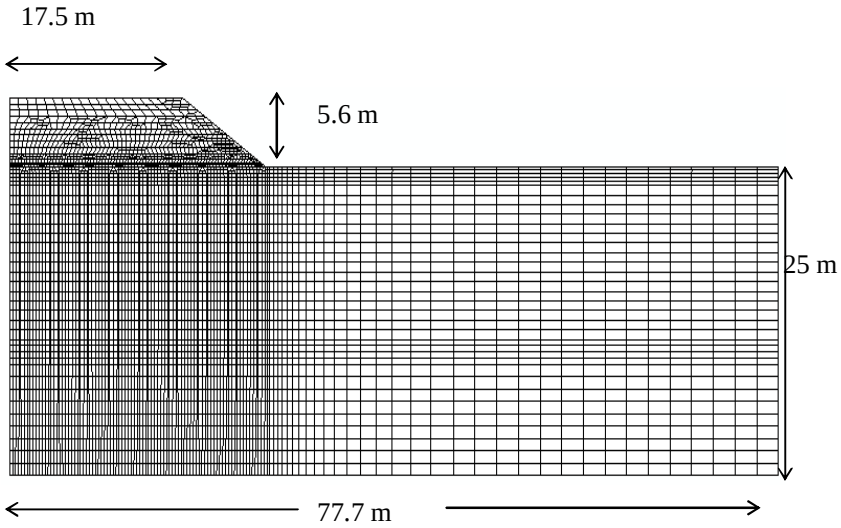

Figure 2: Finite element mesh.

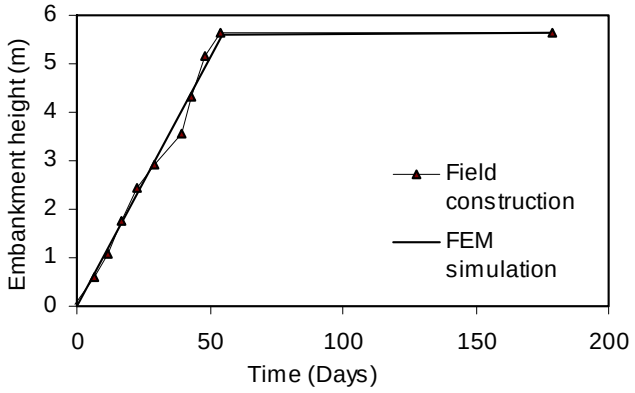

Figure 3: Embankment construction history.

4 LOAD TRANSFER FROM THE EMBANKMENT TO PILES

Figure 4 shows the computed pressure acting on the soil surface between the first and second piles and the second and third piles, where pile numbers are shown in Figure 1. The measured pressure is also shown in Figure 4. Although the pressure acting on soil around the second pile was measured using eight earth pressure cells during the embankment construction, the measured value between first and second piles is shown in Figure 4 because the finite element analysis was carried out assuming plane strain conditions. Also Figure 4 shows the embankment load, γH, where H is the embankment height and γ is the unit weight of the embankment fill material. The computed pressure acting on the foundation soil agrees well with the measured data and the pressure applied on the foundation soil is about 37% of the embankment load.

Table 1: Properties of soil, pile and geosynthetic.

Material	Parameters
Silty clay	$\lambda = 0.06$, $\kappa = 0.012$, $M = 1.2$, $e_1 = 0.87$, OCR = 1, $\nu = 0.35$, $k = 8.64\text{x}10^{-4}$ m/day, $\gamma = 19.8$ kN/m^3
Soft silty clay	$\lambda = 0.15$, $\kappa = 0.03$, $M = 0.95$, $e_1 = 1.79$, OCR = 1, $\nu = 0.4$, $k = 4.32\text{x}10^{-4}$ m/day, $\gamma = 17.3$ kN/m^3
Medium silty clay	$\lambda = 0.05$, $\kappa = 0.01$, $M = 1.1$, $e_1 = 0.88$, OCR = 1, $\nu = 0.35$, $k = 4.32\text{x}10^{-4}$ m/day, $\gamma = 20$ kN/m^3
Sandy silt	$\lambda = 0.03$, $\kappa = 0.005$, $M = 0.28$, $e_1 = 0.97$, OCR = 1, $\nu = 0.35$, $k = 4.32\text{x}10^{-3}$ m/day, $\gamma = 19.8$ kN/m^3
Embankment	$E = 20$ MPa, $c' = 10$ kPa, $\phi' = 30^o$, $\psi = 0$, $\nu = 0.3$, $\gamma = 18.5$ kN/m^3
Gravel	$E = 20$ MPa, $c' = 10$ kPa, $\phi' = 40^o$, $\psi = 0$, $\nu = 0.3$
Coarse grained fill	$E = 7$ MPa, $c' = 15$ kPa, $\phi' = 28^o$, $\psi = 0$, $\nu = 0.3$, $\gamma = 18$ kN/m^3
Pile	$E = 20$ GPa, $\nu = 0.2$
Geosynthetic	$J = Et = 1180$ kN/m, $\nu = 0.3$

J – Stiffness of the Geosynthetic, t – thickness of the Geosynthetic, γ – unit weight of the soil

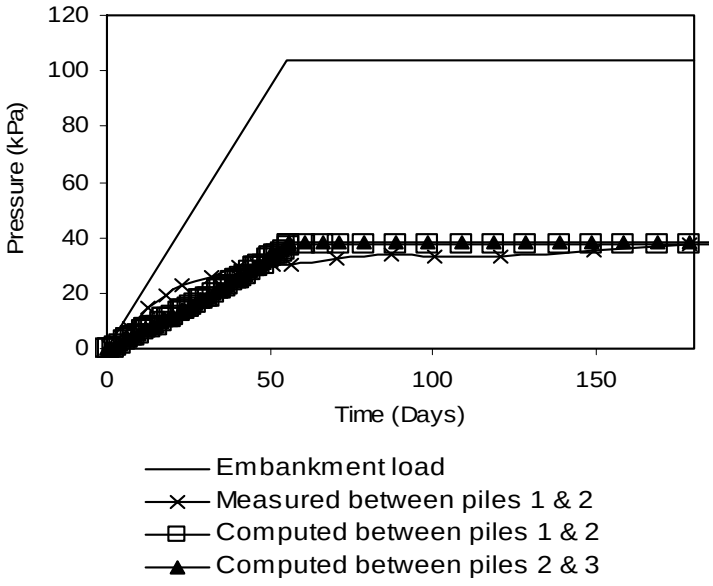

Figure 4: Pressure acting on the soil surface between piles.

Figure 5 shows the pressure acting on pile 2. The average pressure acting on the pile head is 680 kPa, which is about 6.6 times the embankment load. Figure 6 shows the vertical stress acting on the geosynthetic which reaches a maximum of 170 kPa at the pile head and decreases to 40 kPa mid-span between piles, which is nearly 40% of the embankment load. At the mid-span between piles, the vertical pressure acting on the foundation soil and the geosynthetic are nearly the same. These values clearly show that the majority of embankment load is transferred to the piles and only about 40% of the embankment load is transferred to the foundation soil.

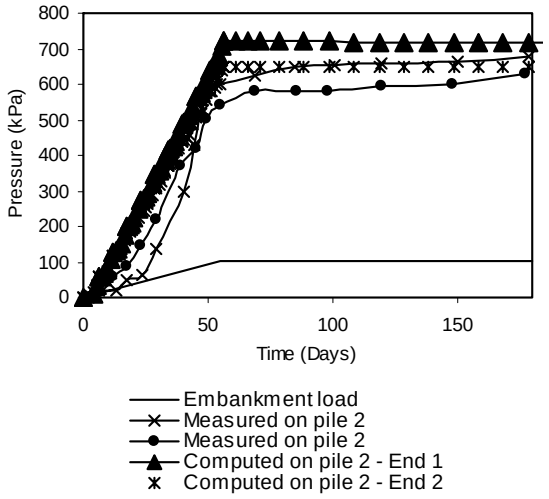

Figure 5: Pressure acting on the piles.

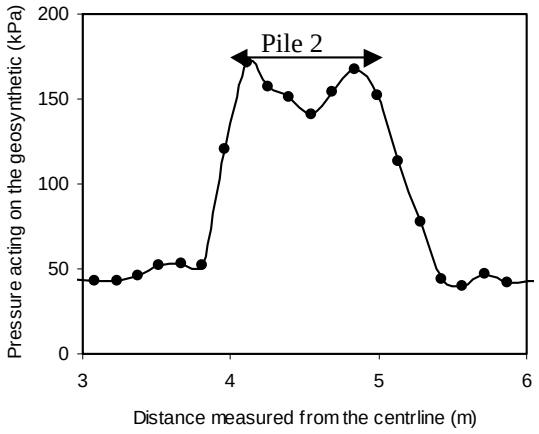

Figure 6: Pressure acting on the geosynthetic (at the end of embankment construction).

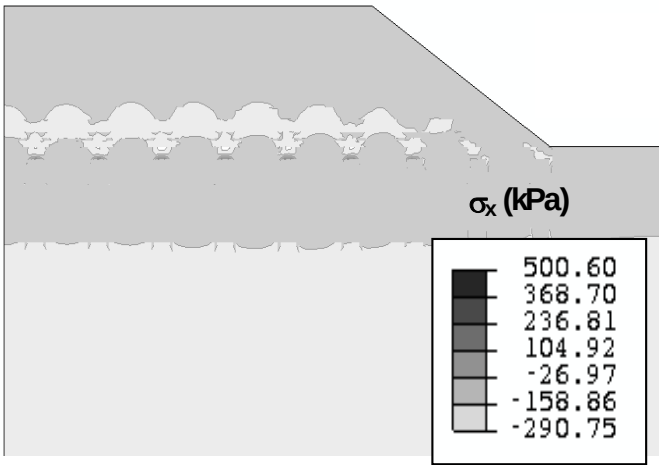

Figure 7. Horizontal stresses above the piles at the end of embankment construction.

Figure 7 shows the horizontal stress distribution within the embankment. This figure clearly illustrates the dome shaped horizontal stress contours in between piles in the fill material. In a vertically loaded arch, the horizontal component of the stress is a constant. Therefore this figure confirms soil arching, with the majority of the embankment load being transferred to the piles.

The load transfer mechanism due to soil arching can be quantified using the stress concentration ratio, which is defined as the ratio between average vertical stress applied on piles to average vertical stress applied on the foundation soil (Liu *et al.* 2007). The computed stress concentration ratio for the problem analysed in this study is about 16.5. Liu *et al.*

(2007) reported a stress concentration ratio of 14 for the same highway embankment, based on the measured data. In the field the pressure acting on foundation soil was computed as the average of pressures measured around the second pile but in this finite element study the pressure was computed based on the average of pressures computed on either side of pile 2, due to the two-dimensional idealisation of the actual three-dimensional problem.

Barksdale and Goughnour (1984) and Greenwood (1991) reported that stress concentration ratios for piled embankments without any geosynthetic reinforcement are typically in the range of 1 to 8. However, they used stone columns as piles. The contrast between stress concentration ratios may be due to the difference in stiffness between pile material and the foundation soil as well as the presence of the geosynthetic in the current study. When geosynthetic reinforcement is used in piled embankments, the vertical component of the tension in the geosynthetic will also contribute to the load transferred to the piles. Hence, the stress concentration ratio for geosynthetic reinforced piled embankments should be higher than that of piled embankments without geosynthetic reinforcement.

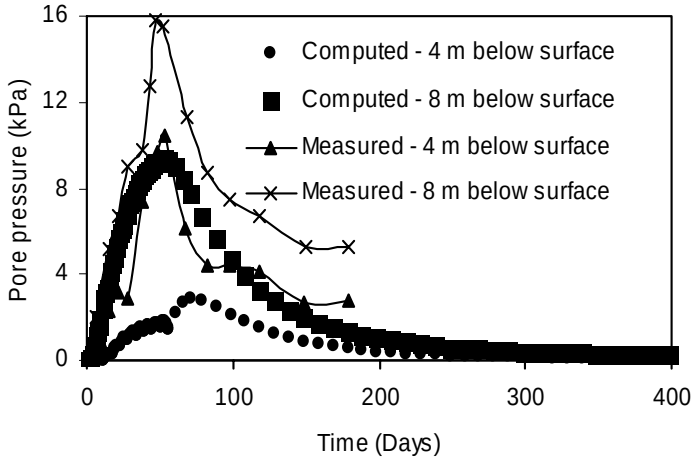

Figure 8: Measured and computed pore pressure between pile 2 and pile 3.

5 VARIATION OF EXCESS PORE PRESSURE

Figure 8 shows the variation of excess pore pressure in the foundation soil between pile 2 and pile 3 at the end of embankment construction, after 55 days, at 4 m and 8 m below the surface. The computed pore pressure at 4 m below the surface, which is closer to the top of the soft silty clay layer and 2.5 m below the zero pore pressure boundary, is about 30% of the measured value. At the 8 m depth, which is closer to the mid-depth of the soft silty clay layer, the measured excess pore pressure is about 60% of that measured. Although piles used in the embankment are cast-in-place piles, a temporary double-wall casing is driven into the ground by a vibrating machine. During this process excess pore pressures may also have been generated in the ground. However, the excess pore pressures computed based on the finite element analysis simulated only the pore pressure generation during embankment construction. This may be the reason for low computed excess pore pressures shown in Figure 8.

Figure 9 shows the excess pore pressure distribution at the end of embankment construction. Excess pore pressure is a maximum beneath the centre of the embankment. Although the increase in surcharge load is about 100 kPa, the computed maximum increase in excess pore pressure in the foundation soil is only about 20 kPa. The relatively small pore pressure increase compared to the increase in surcharge load is due to the load transfer from the embankment to the piles beneath it due to soil arching. The foundation soil is subjected to smaller compressive loads and therefore the pore pressure increase in foundation soil is small. In addition, there will be some excess pore pressure dissipation during the embankment construction, which took 55 days.

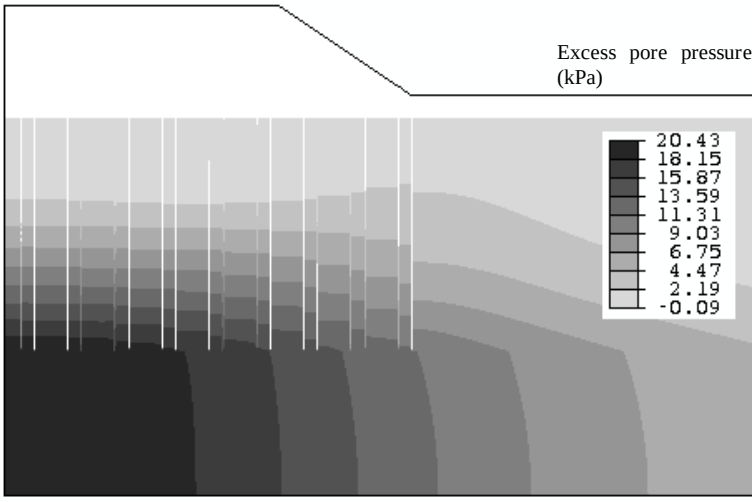

Figure 9: Excess pore pressure distribution in foundation soil at the end of embankment construction.

6 TOTAL AND DIFFERENTIAL SETTLEMENT

Figure 10 shows the computed displacement contours at the end of embankment construction. Closer to the toe of the embankment, the displacements of the soil and piles are comparable. However, when moving towards the center of the embankment, contours show clearly that soil displacements are greater than pile head displacements. This indicates differential settlement at the level of pile heads. However, it has not transferred to the top-of-embankment level.

Figure 11 shows the measured and computed settlements for pile 1 and pile 7. During the period of embankment construction, measured and computed pile settlements agree well. Results show further increase in settlement after embankment construction due to soil consolidation. According to computed settlements, consolidation is complete after about 150 days but the measured results show a rapid increase in settlement due to soil consolidation after the conclusion of the embankment construction. Even after 150 days the actual rate of settlement is significant and has not stabilised. These results indicate that excess pore pressure dissipation is more rapid in the computer simulation compared to that in the field. During consolidation the void ratio of the soil decreases and this will result a decrease in permeability of the soil (Liu *et al.*, 2007). This effect has not been taken into account in the numerical simulation. As a result, the numerical simulation shows too rapid a rate of pore pressure dissipation.

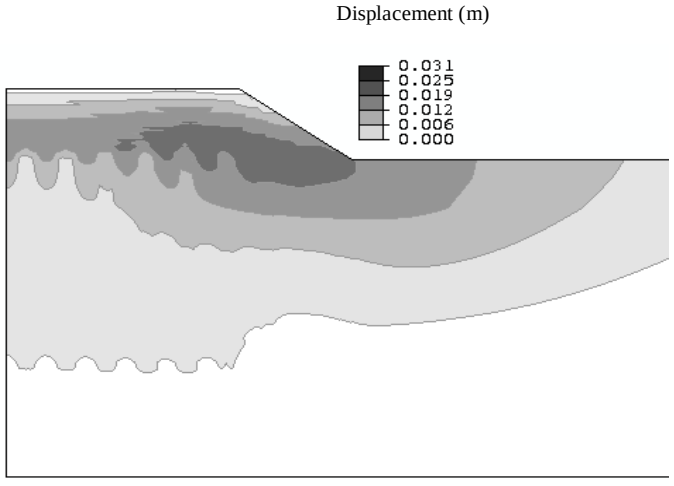

Figure 10: Excess pore pressure distribution in foundation soil at the end of embankment construction.

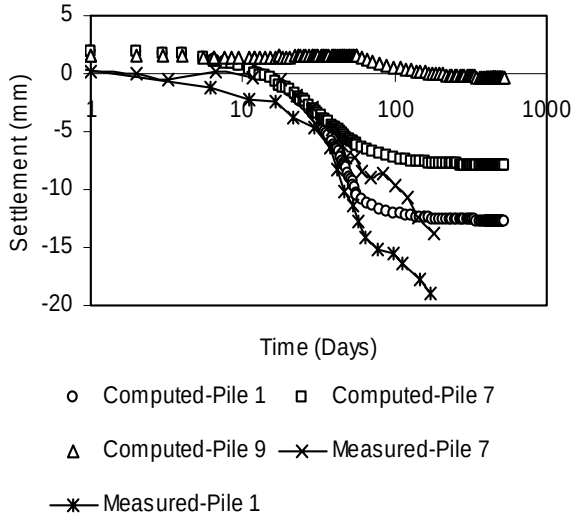

Figure 11. Computed and measured pile settlements.

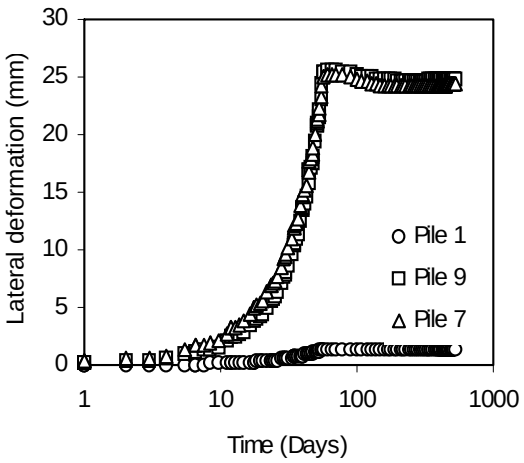

Figure 12. Computed pile lateral deformations.

Figure 11 also shows the settlement of pile 9, which is at the toe of the embankment. Compared to the settlement of pile 7, at the end of consolidation the computed settlement of pile 9 is negligible.

Figure 12 shows computed lateral deformations of pile 1, pile 7 and pile 9. Lateral deformation is critical for the pile closest to the embankment toe and at the end of embankment construction the lateral deformation of the pile closest to the toe is 25 mm. However, the computed lateral deformation is only 1 mm for pile 1. In the current practice used for the design of geosynthetic reinforced piled embankments the lateral effects are not taken into consideration although, within the profession there is general awareness about this issue. Results of this study clearly show that the lateral effects are significant especially for piles and soil closer to the toe of the embankment.

7 ASSESSMENT OF PRACTICAL DESIGN TECHNIQUES

The main difficulty in the design of geosynthetic reinforced pile supported embankments is the calculation of vertical load transferred from the embankment to the geosynthetic, piles and foundation soil. The mechanism of load transfer from the embankment to the geosynthetic is still not well understood, but it is generally assumed that the embankment load is transferred to the piles by the geosynthetic and by soil arching (Russell and Pierpoint, 1997). In this section, four design methods are compared with the finite element results obtained for the case history described in previous sections: BS8006, Terzaghi's arching theory (Terzaghi, 1943), Hewlett and Randolph's arching theory (Hewlett and Randolph, 1988) and Guido *et al.*'s design method (Guido *et al.*, 1987). These methods have been compared using the arching ratio, S, which is defined as,

$$S = \frac{P_r}{\gamma H} \quad \textbf{(1)}$$

where, P_r is the average vertical stress carried by the geosynthetic.

7.1 BS8006 METHOD

The method given in BS8006 has been developed by Jones *et al.* (1990). The load carried by the piles is computed based on the Marston's formula for positively projecting conduits (Russell and Pierpoint 1997). For embankment heights greater than 1.4(*s*-*a*), the distributed load applied on the geosynthetic is given by,

$$P_r = \frac{2.8s\gamma}{(s+a)^2}\left[s^2 - a^2\left(\frac{P_c}{\gamma H}\right)\right] \quad \textbf{(2)}$$

where *s* is the pile spacing, *a* is the pile cap width and,

$$\frac{P_c}{\gamma H} = \left(\frac{C_c a}{H}\right)^2 \quad \textbf{(3)}$$

where C_c is the arching coefficient. For the friction piles used in this study,

$$C_c = 1.5\frac{H}{a} - 0.07 \quad \textbf{(4)}$$

7.2 TERZAGHI'S ARCHING THEORY

Terzaghi (1943) examined soil arching effects using his classical trap door experiment. Russell and Pierpoint (1997) have extended Terzaghi's analysis for piled embankments with geosynthetic. They derived an expression for the distributed load applied on the geosynthetic due to arching given by,

$$P_r = \frac{\left(s^2 - a^2\right)\gamma}{4aK\tan\phi'}\left[1 - e^{\frac{-4aHK\tan\phi'}{\left(s^2-a^2\right)}}\right] \quad \textbf{(5)}$$

where K is the coefficient of earth pressure at rest. For normally consolidated soils, K can be related to the effective friction angle of the soil ϕ' by,

$$K = 1 - \sin\phi' \quad \textbf{(6)}$$

7.3 HEWLETT AND RANDOLPH'S ARCHING THEORY

For the pile-supported embankment systems, Hewlett and Randolph (1988) carried out model tests and observed the formation of vaults across adjacent pile caps and developed expressions to obtain the load carried by piles. In the design, it is assumed that the proportion of the embankment load that has not been transferred on to the pile caps has been supported by the geosynthetic. The critical location for the vertical stress is either at the crown of the arch or at the pile. The average pressure applied on the geosynthetic based on the conditions at the crown of the arch is given by (Russell and Pierpoint 1997),

$$P_r = \gamma H\left(1 - \frac{a}{s}\right)^{2(k_p - 1)}\left[1 - \frac{s}{\sqrt{2}H}\frac{2(K_p - 1)}{(2K_p - 3)}\right] + \frac{(s-a)}{\sqrt{2}H}\frac{2(K_p - 1)}{\left(2K_p - 3\right)} \quad \textbf{(7)}$$

Based on the conditions at the pile, average pressure applied on the geosynthetic is given by,

$$P_r = \frac{\gamma H}{\left(\frac{2K_p}{K_p + 1}\right)\left[\left(1 - \frac{a}{s}\right)^{(1-K_p)} - \left(1 - \frac{a}{s}\right)\left(1 + \frac{a}{s}K_p\right)\right] + \left(1 - \frac{a^2}{s^2}\right)} \quad \textbf{(8)}$$

where K_p is the passive earth pressure coefficient. Usually the higher of the values given by Equations 7 or 8 is used in the design.

7.4 GUIDO *ET AL.*'S METHOD

The design for the Second Severn Crossing embankment in the UK used Guido's method (Russell and Pierpoint 1997). In this method it is assumed that a rectangular pyramid of fill material above the geosynthetic spanning between piles is transferred to the geosynthetic. Then the load carried by the geosynthetic is given by,

$$P_r = \frac{\gamma\left(s - a\right)}{3\sqrt{2}} \quad \textbf{(9)}$$

Figure 13 compares the values of arching ratio obtained from the design methods described in this section. This figure clearly shows the inconsistencies in different methods. Finite element analysis results in an arching ratio of 0.5 whereas BS8006 gives an arching ratio of 0.99, which indicates no soil arching for the example problem. Terzaghi's arching theory and Hewlett and Randolph's method yield similar arching ratios closer to 0.8. However, Guido *et al.*'s method provides an arching ratio of 0.1, which is the lowest.

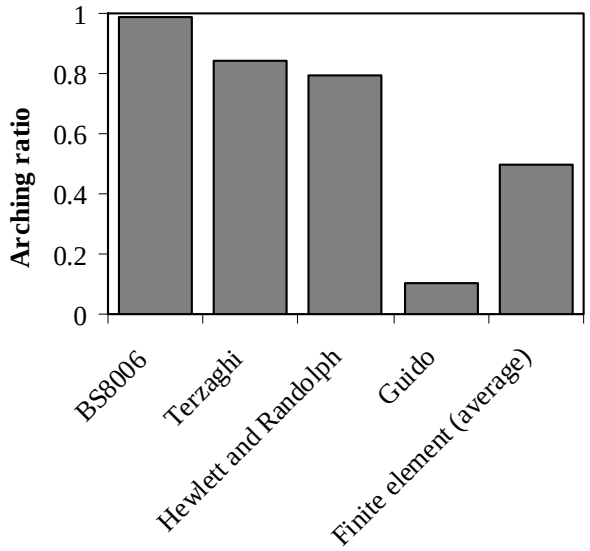

Figure 13: Comparison of different design methods.

The domes of constant horizontal stress illustrated in Figure 7, based on the finite element analysis, clearly demonstrate soil arching and are consistent with an arching ratio of 0.5 obtained from the finite element analysis. Therefore it can be concluded that the BS8006 over-predicts the arching ratio. On the other hand Guido's method under-predicts the soil arching ratio for a geosynthetic reinforced piled-embankment. Terzaghi's method and Hewlett and Randolph's method use arching theory. Therefore, they yield comparable arching ratios but they do not agree with the finite element results as both methods are developed without incorporating geosynthetic reinforcement.

8 CONCLUSION

A numerical study has been carried out to investigate the load transfer mechanism in geosynthetic reinforced pile supported embankments. Results show that the majority of embankment load is carried by the piles due to the soil arching effect. The lateral effects have a significant influence on the performance of the embankment, even though they are not incorporated in current practice. Finite element results have been compared with four design techniques used in practice and the comparisons clearly demonstrate the inconsistencies in current practice.

9 REFERENCES

Barksdale, R.D. and Goughnour, R.R. 1984. Performance of a stone column supported embankment. *Proc. Int. Conf. On Case Histories in Geotechnical Engineering,* St. Louis, 6-11.

Greenwood, D.A. 1991. Load tests on stone columns. *Proc. Deep Foundation Improvements: Design, Construction and Testing,* ASTM, Philadelphia, 148-171.

Guido, V.A., Kneuppel, J.D. and Sweeney, M.A. 1987. Plate loading tests on geogrid reinforced earth slabs, *Proc. of the Geosynthetics '87,* New Orleans, 216-225.

Han, J. and Akins, K. 2002. Use of Geogrid-reinforced and pile-supported earth structures, *Proceedings of the International Deep Foundation Congress,* ASCE, 668-679.

Hewlett, W.J. and Randolph, M.F. 1988) Analysis of piled embankments, *Ground Engineering,* 21(3): 12-18.

Jones, C.J.F.P., Lawson, C.R. and Ayres, D.J. 1990) Geotextile reinforced piled embankments, *Proc. of the 4th International Conference on Geotextiles, Geomembranes and Related Products*, Balkema, Rotterdam, 155-160.

Liu, H.L., Ng, C.W.W. and Fei, K. 2007. Performance of a geogrid reinforced and pile supported highway embankment over soft clay: Case study, *Journal of Geotechnical and Geoenvironmental Engineering,* ASCE, 133(12): 1483-1493.

Russell, D. and Pierpoint, N. 1997. An assessment of design methods for piled embankments, *Ground Engineering*, November, 39-44.

Terzaghi, K. 1943. *Theoretical Soil Mechanics,* John Wiley & Sons, New York.